Modified matched signal transform for parameter estimation of spread spectrum stretch signal

XIAODONG ZENG
Southwest China Institute of Electronic Technology
No.85, West YingKang Road, Chengdu
CHINA
zengxdcetc@sina.cn

Abstract: - The spread spectrum stretch (S-cubed) is a kind of hybrid signal which has the advantages of the expansion and wide instantaneous bandwidth, proved to be the potential option for low probability of intercept (LPI) radar and stealth communications. In this paper, the S-cubed model that superimposes a short, cyclically repeated, discrete phase code on linear frequency modulation (LFM) is presented. In order to extract the signal features, we formulate modified matched signal transform (MMST) and then propose a novel approach to estimate the parameters of S-cubed in MMST domain. Furthermore, the numerical simulation and parameter estimation robustness are also studied. The simulation results show that when signal to noise ratio (SNR) is -7dB, the probability of correct decision (PCD) of the chirp rate has reached 90%.

Key-Words: - spread spectrum stretch (S-cubed); modified matched signal transform (MMST); parameter estimation.

1 Introduction

Over the past decade, the hybrid modulation approach has been widely used in radar and communications [1-4]. It improves a tracking performance criterion such as minimizing the tracking mean-squared error (MSE) or maximizing target information retrieval. Furthermore, it has raised an unprecedented challenge to electronic reconnaissance because of the unpredictability and randomness. The spread spectrum stretch (S-cubed) studied here is a novel hybrid signal which simultaneously exploits linear frequency modulation (LFM) and discrete phase code [5]. The hybrid S-cubed is fast becoming an important method applied in low probability of intercept (LPI) radar and stealth communications because it has the advantages of these two kinds of modulations which are the expansion performance of LFM and wide instantaneous bandwidth of discrete phase code. Meanwhile, the synergistic effects of combining LFM and discrete phase code can further reduce the probability of intercept to electronic reconnaissance.

According to the square phase of LFM and the superposition phase shift of discrete phase code, the S-cubed has the characteristic of nonlinear phase. Under the circumstances, matched signal transform (MST) becomes a potential transform to process the S-cubed. MST can effectively extract nonlinear phase signal characteristics in MST domain. Chetwani [6] introduces the principle of MST which has been applied in communication system to remove the time-varying interference. It is perfectly localized at the FM rate of signals with linear or non-linear instantaneous frequency in the time-frequency domain. Shen [7] studies the interference suppression of the direct sequence spread spectrum (DSSS) communication system through MST. MST is highly localized for signals with nonlinear phase along their modulation rate. Li [8] employs MST to identify smeared spectrum (SMSP) jamming in radar system. The new algorithm of jamming recognition based on MST obtains a fairly high correct identification ratio. MST is widely used in various fields. It is available to remove the interference, identify the jamming and estimate the parameter.

Motivated by MST, the modified MST (MMST) pointing for the S-cubed is proposed. First, we compare the MMST of S-cubed with that of LFM and deduce their relativity. Secondly, employing the S-cubed signal feature in MMST domain, the chirp rate of the single and multi-components can be obtained. In the light of the estimated chirp rate, we reconstruct the original LFM signal and then use this signal to de-chirp the S-cubed leaving discrete phase code. Finally, by the cyclic autocorrelation function of the code, the code rate is also estimated. When the signal to noise ratio (SNR) is -7dB, the probability of correct decision (PCD) of the chirp rate by the proposed algorithm has reached 90%.

Meanwhile, when the SNR is more than 6dB, the normalized root mean square error (NRMSE) of the estimated code rate is less than 10^{-2}.

2 The Signal Model

The S-cubed is a signal that simultaneously contains two kinds of modulations, LFM and discrete phase code. It not only has the advantageous processing property of stretch but also gains wide instantaneous bandwidth of discrete phase code. The S-cubed can be denoted as

$$S_c(t)=\sum_{l=1}^{L}A_l\frac{1}{\sqrt{NP}}\sum_{n=0}^{N-1}\sum_{p=0}^{P-1}e^{j\sum_{d=0}^{D}a_d^l t^d}\,c_p\mu\left[\left(t-pT_1-nT_2\right)/T_1\right] \quad (1)$$

where $\mu(t)=\begin{cases}1, 0\le t<1\\ 0, otherwise\end{cases}$, P is the code length, usually a small integer, such as 4. N is the number of repeated periods. T_1 and T_2 are the code width and the period, respectively. $T_2=PT_1$. c_p is the code, $c_p\in\{-1,1\}$ when it is binary discrete phase code, $c_p\in\{-1,1,-j,j\}$ when it is Frank code. A_l is the signal amplitude, d the polynomial phase order, D the maximum. $a_d^{\ l}$ is the coefficient of lth-component, L the number of components. Of course, there are a variety of polynomial phase candidates, but undoubtedly, LFM is a mature technique which might be used. In this paper, we focus on the square phase of LFM, then $[a_1^{\ l}a_3^{\ l}...a_D^{\ l}]=0$.

In particular, Lynch [5] points out that, different from the traditional phase codes, discrete phase code of the S-cubed needs to have the minimal mismatch loss in decoding and optimal spectral spreading. At present, there are several kinds of potential discrete phase codes alternative, such as binary phase code with length 4 and Frank code with length 16. This paper assumes that waveform designers adopt binary phase code with length 4 which is more common and easier for realization. The length 4 code is the binary phase code with no mismatch loss; i.e., the mismatch loss

$$L=10\log_{10}\left[\left(\sum_{p=0}^{P-1}c_p\omega_p\right)^2\Big/\left(P\bullet\sum_{p=0}^{P-1}\left|\omega_p\right|^2\right)\right] \quad (2)$$

where $c_p=\omega_p=[1\quad 1\quad -1\quad 1]$, ω_p the decoder weightings, then $L=0$ dB.

Meanwhile, the instantaneous signal power spread uniformly over $1/T_1$ producing close to a LPI improvement $P=10\log_{10}\left(\left|\sum_{p=0}^{P-1}c_p\right|^2/P^2\right)=-6dB$ for an interceptor detection filter with the bandwidth of $1/PT_1$ relative to conventional stretch.

A code of length 4, with a 25 ns code width, generates a line spectrum with lines $1/(4\times 25\text{ns})=10$MHz apart.

With 10 MHz channelized receiver filter, the long code width which is beyond four 25 ns chips will put more lines in each detection filter. However, a detection filter designed for conventional stretch could be much narrower than 10 MHz, and then a longer code would be effective. A near-uniform spreading of the instantaneous signal power over $1/T_1$=40MHz produces close to a 6 dB LPI improvement for a 10 MHz interceptor detection filter, relative to conventional stretch.

In summary, the S-cubed approach has the instantaneous bandwidth properties of discrete phase code, along with the highly desirable sampling and data rate properties of stretch. All of these properties make it be applied in a wide field, such as LPI radar and stealth communications.

3 The Parameter Estimate of The S-cubed Based on MMST

Neither the time domain nor frequency domain can adequately reflect its characteristics. The time-frequency transform can be used to study it naturally [9]. Based on the phase difference, we can also extract the instantaneous frequency and estimate the parameters [10]. The methods above are feasible, but time-frequency approach incurs large amount of calculation and the phase difference is sensitive to the noise. This paper focuses on the composition of S-cubed and extracts the signal features in the MMST domain. The following results show that the proposed method can be implemented by FFT to cut the computation load and is effective in the negative SNR.

MST can be denoted as [6-7]

$$F(f_g)=\int_{t\in t_c}[S_c(t)/g(t)]e^{-j2\pi f_g\xi(t)}dt \quad (3)$$

where $\xi(t)$ is the nonlinear characteristic basis function. $g(t)=1/\sqrt{|d\xi(t)/dt|}$. t_c is the observation time of $\xi(t)$. f_g is the frequency in MST domain.

$\xi(t)$ is selectable such as Mellin, linear, power and exponential basis functions. Among them, there is an important MST which adopts the linear basis function called linear MST (LMST). LMST is ideally matched to LFM signal.

3.1 MMST of the S-cubed

Since the S-cubed combines LFM, LMST is the preferential choice for its feature extraction. But the S-cubed also includes discrete phase code resulting in an effect on the linearity of LMST. The linearity is useful for the electronic reconnaissance signal processing because it occurs sometimes that the receiver intercepts the time-frequency overlapped S-cubed signals in the complex electromagnetic environment. In such a case, we should exploit the linearity of LMST to separate them from the transform domain. For this reason, we do some modifications to LMST and get the derivative MMST which maintains the linearity for the S-cubed.

$$F_{3s}(f_g)=\int_{t\in t_c}[S_c(t)/g_\alpha(t)]e^{-j2\pi f_g\xi(t)}dt \quad (4)$$

where $g_\alpha(t)=1/(\alpha\cdot d\xi(t)/dt)$ and α is the linear factor. $\xi(t)=0.5t^2$ and $\alpha=2$.

3.1.1 Single component case

For MMST of the S-cubed, we consider the single component signal with $a_0=\varphi_0$ and $a_2=\pi k$.

$$S_c(t)=\frac{1}{\sqrt{NP}}\sum_{n=0}^{N-1}\sum_{p=0}^{P-1}e^{j(\pi kt^2+\varphi_0)}c_p\mu\left[\left(t-pT_1-nT_2\right)/T_1\right] \quad (5)$$

where k and φ_0 are the chirp rate and initial phase, respectively. Assuming that there are two codes with phase discontinuity 0 to π in the observation time $[t_1,t_2]$, t_0 is the cut-off time. MMST of the S-cubed arrives at

$$F_{3s}(c)=\int_{t_1}^{t_0}(e^{j\pi kt^2}\cdot 2t)e^{-j\pi f_g t^2}dt-\int_{t_0}^{t_2}(e^{j\pi kt^2}\cdot 2t)e^{-j\pi f_g t^2}dt \quad (6)$$

Make $u_1\left(t_1'\right)=\begin{cases}1, t_1^2<t_1'<t_0^2\\ 0, otherwise\end{cases}$

and $u_2\left(t_2'\right)=\begin{cases}1, t_0^2<t_2'<t_2^2\\ 0, otherwise\end{cases}$, then

$$\begin{aligned}F_{3s}(c)&=\int_{-\infty}^{\infty}u_1(t_1')e^{j\pi ct_1'}dt_1'-\int_{-\infty}^{\infty}u_2(t_2')e^{j\pi ct_2'}dt_2'\\&=\frac{2\sin[\pi c(t_0^2-t_1^2)/2]}{\pi c}e^{-j\pi c(t_0^2+t_1^2)/2}\\&\quad-\frac{2\sin[\pi c(t_2^2-t_0^2)/2]}{\pi c}e^{-j\pi c(t_0^2+t_2^2)/2}\end{aligned} \quad (7)$$

According to Euler's theorem

$$\begin{aligned}F_{3s}(c)&=\frac{1}{j\pi c}[\cos(\pi ct_0^2)-\cos(\pi ct_1^2)\\&\quad+\cos(\pi ct_0^2)-\cos(\pi ct_2^2)]\\&\quad+\frac{1}{\pi c}[\sin(\pi ct_0^2)-\sin(\pi ct_1^2)\\&\quad+\sin(\pi ct_0^2)-\sin(\pi ct_2^2)]\\&=\frac{2j}{\pi c}\left\{\begin{aligned}&\sin[\pi c(t_0^2+t_1^2)/2]\sin[\pi c(t_0^2-t_1^2)/2]\\&+\sin[\pi c(t_0^2+t_2^2)/2]\sin[\pi c(t_0^2-t_2^2)/2]\end{aligned}\right\}\\&\quad+\frac{2}{\pi c}\left\{\begin{aligned}&\cos[\pi c(t_0^2+t_1^2)/2]\sin[\pi c(t_0^2-t_1^2)/2]\\&+\cos[\pi c(t_0^2+t_2^2)/2]\sin[\pi c(t_0^2-t_2^2)/2]\end{aligned}\right\}\end{aligned} \quad (8)$$

where $c=k-f_g$.

The modulus of MMST spectrum from (8) is

$$\begin{aligned}|F_{3s}(c)|&=\frac{2}{\pi|c|}\cdot\\&\sqrt{\begin{aligned}&\sin^2[\pi c(t_0^2-t_1^2)/2]+\sin^2[\pi c(t_0^2-t_2^2)/2]\\&+2\sin[\pi c(t_0^2-t_1^2)/2]\sin[\pi c(t_0^2-t_2^2)/2]\cdot\\&\cos[\pi c(t_1^2-t_2^2)/2]\end{aligned}}\end{aligned} \quad (9)$$

Compared with the S-cubed, we also get MMST of the LFM.

$$F_{LFM}(c)=\frac{1}{j\pi c}[\cos(\pi ct_2^{\,2})-\cos(\pi ct_1^{\,2})]$$
$$+\frac{1}{\pi c}[\sin(\pi ct_2^{\,2})-\sin(\pi ct_1^{\,2})]$$
$$=\frac{2j}{\pi c}\left\{\sin[\pi c(t_2^{\,2}+t_1^{\,2})/2]\sin[\pi c(t_2^{\,2}-t_1^{\,2})/2]\right\}$$
$$+\frac{2}{\pi c}\left\{\cos[\pi c(t_2^{\,2}+t_1^{\,2})/2]\sin[\pi c(t_2^{\,2}-t_1^{\,2})/2]\right\} \quad (10)$$

The modulus of MMST spectrum from (10) is

$$\left|F_{LFM}(c)\right|=\frac{2}{\pi|c|}\left|\sin[\pi c(t_2^{\,2}-t_1^{\,2})/2]\right|$$
$$=\frac{2}{\pi}\left|\frac{\sin[\pi c(t_2^{\,2}-t_1^{\,2})/2]}{c}\right| \quad (11)$$

From the equation (9) and (11), we observe that MMST of the S-cubed has an additional term to that of LFM. The additional term which results from discrete phase code is

$$F_a=\frac{2}{\pi|c|}\cdot\sqrt{2\sin[\pi c(t_0^{\,2}-t_1^{\,2})/2]\sin[\pi c(t_0^{\,2}-t_2^{\,2})/2]}\cdot\sqrt{\cos[\pi c(t_1^{\,2}-t_2^{\,2})/2]} \quad (12)$$

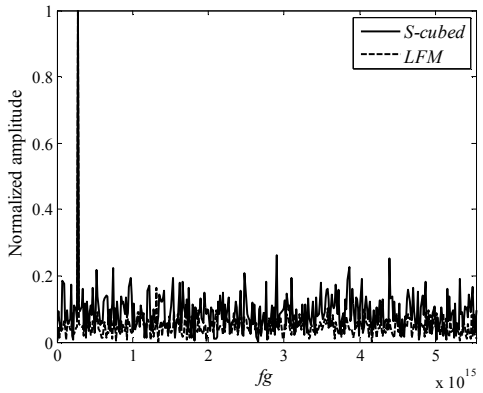

Fig. 1 The modulus of MMST spectrum for the single component

Fig.1 shows the modulus of MMST spectrum. In Fig.1, 'S-cubed' stands for MMST of the S-cubed, 'LFM', MMST of LFM. There is a peak for $\left|F_{3s}(c)\right|$ and $\left|F_{LFM}(c)\right|$ at $c=0$. The side lobes of the S-cubed are worse than the LFM because of the phase discontinuity caused by discrete phase code.

3.1.2 Multi-components case

Based on the linearity of MMST, when the $S_c(t)$ consists of multiple components

$$S_c(t)=\sum_{l=1}^{L}A_l\frac{1}{\sqrt{NP}}\cdot\sum_{n=0}^{N-1}\sum_{p=0}^{P-1}e^{j\left(\pi k_l t^2+\varphi_l\right)}c_p\mu\left[\left(t-pT_1-nT_2\right)/T_1\right] \quad (13)$$

then

$$MMST[S_c(t)]=MMST[S_c^{\,1}(t)]+MMST[S_c^{\,2}(t)]+\ldots+MMST[S_c^{\,L}(t)] \quad (14)$$

where $MMST[\cdot]$ is MMST operator. $S_c^{\,l}(t)=A_l\frac{1}{\sqrt{NP}}\sum_{n=0}^{N-1}\sum_{p=0}^{P-1}e^{j\left(\pi k_l t^2+\varphi_l\right)}c_p\mu\left[\left(t-pT_1-nT_2\right)/T_1\right]$ is the lth-component.

3.1.3 Fast algorithm

Considering the fast algorithm of (3), we make that $t_\xi=\xi(t)$, then $t=\xi^{-1}(\xi(t))=\xi^{-1}(t_\xi)$ and $dt=\alpha g_\alpha(t)dt_\xi$. Thus, (3) can be rewritten as

$$F_{3s}(f_g)=\int_{t_\xi\in t_c'}S_{conv}(t_\xi)e^{-j2\pi f_g t_\xi}dt_\xi \quad (15)$$

where $S_{conv}(t_\xi)=\alpha S(\xi^{-1}(t_\xi))$ is the convolution signal. t_c' is the observation time of $S_{conv}(t_\xi)$. From (15), we find out that there are two main steps to realize MMST. First, we get the convolution signal $S_{conv}(t_\xi)$ and then estimate the frequency of $S_{conv}(t_\xi)$ in the transform domain by FFT.

3.2 Parameter estimation

From equation (9) and Fig.1, we know that there is a peak for $\left|F_{3s}(c)\right|$ at $c=0$, i.e. $f_g=k$. The location of the peak indicates the chirp rate of the S-cubed. Obviously, we can search for the maximum modulus of MMST, and the corresponding f_g is the estimate of k.

Moreover, we reconstruct the original LFM signal $\hat{S}_{LFM}(t)$ by the above estimate of k.

$$\hat{S}_{LFM}(t)=e^{j\left(\pi\hat{k}t^2\right)} \quad (16)$$

Multiply the conjugation of $S_c(t)$ with $\hat{S}_{LFM}(t)$, we get

$$S(t)=S_c(t)^*\cdot\hat{S}_{LFM}(t)$$
$$=\frac{1}{\sqrt{NP}}\sum_{n=0}^{N-1}\sum_{p=0}^{P-1}e^{j\left(\pi\Delta k t^2-\varphi_0\right)}e^{-j\varphi_p}\mu\left[\left(t-pT_1-nT_2\right)/T_1\right] \quad (17)$$

where φ_p is the code phase corresponding to c_p. Because $\Delta k=\hat{k}-k\approx 0$, $S(t)$ is approximately equal to discrete phase code. The code is repeated cyclically, without loss of generality, we consider the code in one period.

$$S(t)=\frac{1}{\sqrt{P}}\sum_{p=0}^{P-1}e^{-j(\varphi_0+\varphi_p)}\mu\left[\left(t-pT_1\right)/T_1\right] \quad (18)$$

The modulus of the cyclic autocorrelation function $R_S^{\alpha}(\tau)$ [11] is

$$\left|R_S^{\alpha}(\tau)\right|=\begin{cases}\dfrac{\sin(\pi\alpha(\sqrt{P}T_1-|\tau|))}{\pi\alpha\sqrt{P}T_1}, & \alpha=\dfrac{l}{T_1}\\ 0, & otherwise\end{cases} \quad (19)$$

where

$R_S^{\alpha}(\tau)=E[S(t+\frac{\tau}{2})S^*(t-\frac{\tau}{2})\exp(-j2\pi\alpha t)]$ is independent on the initial phase φ_0, α the cycling frequency, l an integer, $|\tau|\neq 0$.

From (19), it is found that $\left|R_S^{\alpha}(\tau)\right|$ is nonzero when the cycling frequency α is an integral multiple of the code rate. Fig.2 shows the spectrum $\left|R_S^{\alpha}(\tau)\right|$. $\left|R_S^{\alpha}(\tau)\right|$ is a discrete spectrum having the peaks when the horizontal axis $\alpha=\dfrac{l}{T_1}$. So, search the peaks of the spectrum $\left|R_S^{\alpha}(\tau)\right|$, then compute the interval between the adjacent peaks which is the estimate of the code rate. However, $\left|R_S^{\alpha}(\tau)\right|$ is the spectrum under multidimensional index. In order to reduce the calculation amount, we should choose a suitable time delay τ_{best} and descend the procedure to one dimension. τ_{best} will be discussed in section 4.2 which is proved to be half of the code width T_1 approximately.

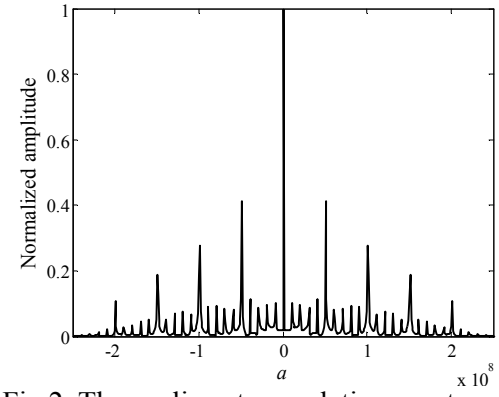

Fig.2 The cyclic autocorrelation spectrum

In conclusion, the procedure of the parameter estimation is shown as follows.

Step 1: Compute the convolution signal $S_{conv}(t_\xi)$.

$$S_{conv}(t_\xi)=\alpha\delta(\xi^{-1}(t_\xi))$$
$$=\alpha\delta(\sqrt{2t_\xi}) \quad (20)$$
$$=\alpha\frac{1}{\sqrt{NP}}\sum_{n=0}^{N-1}\sum_{p=0}^{P-1}e^{j\left(2\pi k t_\xi+\varphi_0\right)}c_p\mu\left[\left(\sqrt{2t_\xi}-pT_1-nT_2\right)/T_1\right]$$

As a result, $S_{conv}(t_\xi)$ becomes a phase shift keying (PSK) signal which has the carrier frequency k. There are many ways to estimate the frequency. FFT is absolutely the direct method. More important, FFT can satisfy the linearity of MMST.

Step 2: Make the FFT of $S_{conv}(t_\xi)$ to obtain MMST spectrum whose horizontal axis is h, $0.5T_c^2 f_g+1=h$, T_c is the pulse duration.

Step 3: In MMST domain, search for the maximum denoted as $\left|F_{3s}(h)\right|_{\max}$ and record the corresponding index $h_{\max}$. Then

$$\hat{k}=\frac{h_{\max}-1}{\xi(T_c)}=\frac{h_{\max}-1}{0.5T_c^2} \quad (21)$$

From (21), of course, we know the frequency resolution of $\hat{k}$ that is $\dfrac{1}{\xi(T_c)}$. Both the nonlinear characteristic basis function and pulse duration have an effect on the frequency resolution which will be studied at section 4.3.

Step 4: De-chirp the S-cubed by the reconstructed LFM signal $\hat{S}_{LFM}(t)$ to obtain discrete phase code.

Step 5: Calculate the cyclic autocorrelation $\left|R_S^{\alpha}(\tau)\right|$ of discrete phase code, and then search the peaks of the spectrum $\left|R_S^{\alpha}(\tau)\right|$ getting the code rate estimate.

4 Simulations

In order to test the proposed algorithm, the following simulations are done. In simulations, the sampling frequency f_s=1GHz, code length $P=4$, code width $T_1=15ns$, and discrete phase code is [1 1 -1 1]. The bandwidth is 100MHz. The time of Monte Carlo is 1000. For the single component, the chirp rate $k=B/(N\cdot P\cdot T_1)$, and the proposed algorithm is compared with the dual threshold method. For the dual threshold method, when SNR is more than 7dB, the threshold $D=10$; otherwise, $D=8$. Aiming at the situation of four components, chirp rates $k_1=B/(N\cdot P\cdot T_1)$, $k_2=2k_1$, $k_3=3k_1$, $k_4=4k_1$. When the error of the chirp rate estimate $\frac{k-\hat{k}}{k}$ is less than 0.1%, it is regarded as one correct decision where $\hat{k}$ is the estimate of k. The performance is evaluated by the PCD. The PCD is defined as the ratio of the number of correct decisions to the total time of Monte Carlo. For the estimate of the code rate, the NRMSE is the criteria. The definition of NRMSE is as follows

$$NRMSE=\frac{\sqrt{\frac{1}{M_o}\sum_{v=1}^{M_o}\left(x_v-x\right)^2}}{x} \tag{22}$$

where x is the parameter to be estimated, x_v is the estimate in the *vth* time. M_o is the time of Monte Carlo.

4.1 The chirp rate estimation

Through the analysis of section 3.1, when the phase function of the S-cubed matches the nonlinear characteristic basis function $\xi(t)$, a peak will appear at $f_g=k$. As a result, the chirp rate of the S-cubed could be estimated by the sharp spectral peak in MMST domain. When the chirp rate is estimated by MMST spectrum, the observation time is $(-\infty,+\infty)$ theoretically so that the spectral peak of MMST has the Dirac function form. In practice, the observation time is limited that is equivalent to add the window in the time domain. The introduction of window functions increases the side lobes and reduces the peak amplitude. However, it only needs to get the accurate position of the main lobe. The influence of the amplitude precision can be ignored, so the rectangular window is the potential choice.

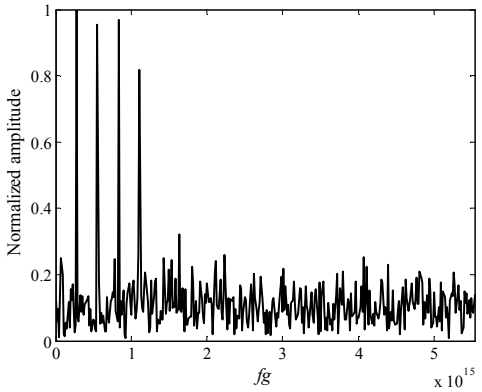

Fig. 3 The modulus of MMST spectrum for the four components

Fig.3 shows the modulus of MMST spectrum of four components. There are four peaks corresponding to four components. The locations of these peaks are related to the chirp rates.

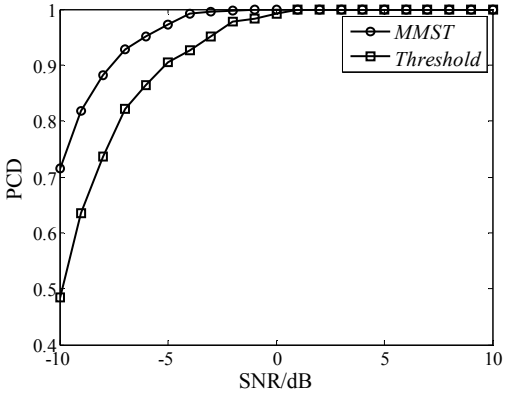

(a) single component

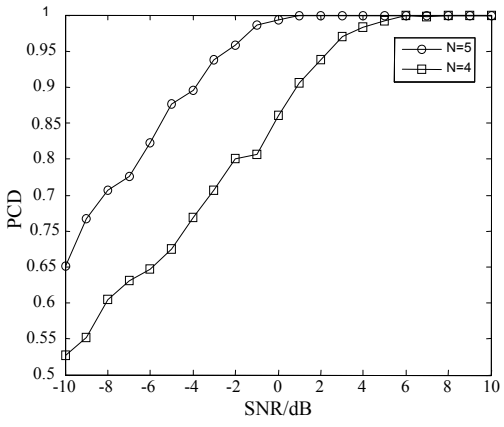

(b) double components of k_1

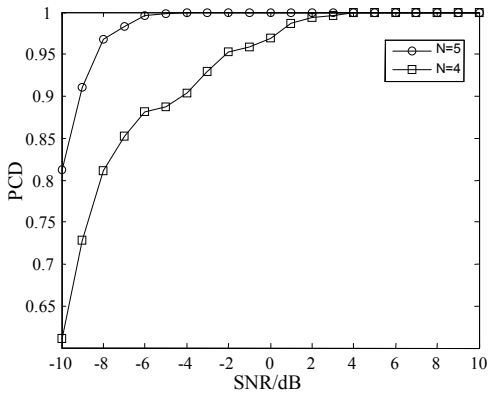

(c) double components of k_2

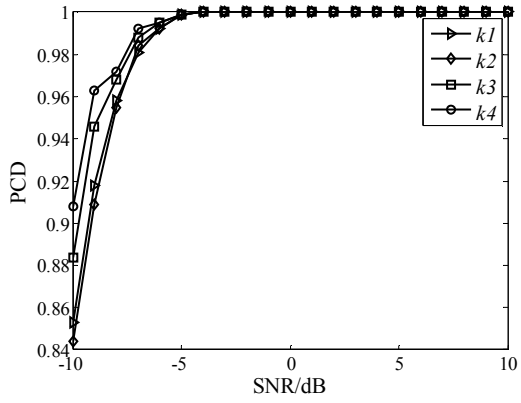

(d) four components

Fig. 4 PCD VS SNR of the chirp rate

In Fig.4, 'MMST' stands for the single component by MMST, 'Threshold' the single component by the dual threshold method. 'N' period number. 'k1', 'k2', 'k3' and 'k4', the four components by MMST.

From the simulations above we can know that when the SNR is -7dB, the PCD of the chirp rate by the proposed algorithm has reached 90%, however, for the dual threshold method, in order to reach the same probability, the minimum SNR needed is -5dB.

In order to study the adaptability for the multi-components, simulations are made for four components signal. The simulation results prove the linearity of MMST for the S-cubed. The multi-components present multiple peaks in MMST domain. The high PCD of the chirp rate can be accomplished via locating the peaks.

4.2 The code rate estimation

Table 1 NRMSE of the code rate estimation

NRMSE (10^{-1})	The choice of the time delay		
	$0.3T_1$	$0.6\ T_1$	$0.5\ T_1$
SNR=2dB	0.751	0.561	0.339
SNR=4dB	0.595	0.265	0.136
SNR=6dB	0.306	0.039	0.039
SNR=8dB	0.173	0.039	0.039
SNR=10dB	0.039	0.039	0.039
SNR=12dB	0.039	0.039	0.039
SNR=14dB	0.039	0.039	0.039
SNR=16dB	0.039	0.039	0.039
SNR=18dB	0.039	0.039	0.039

Table 1 shows the NRMSE of code rate estimation by different time delays. The simulation results indicate that τ_{best} is a half of the code width T_1 approximately.

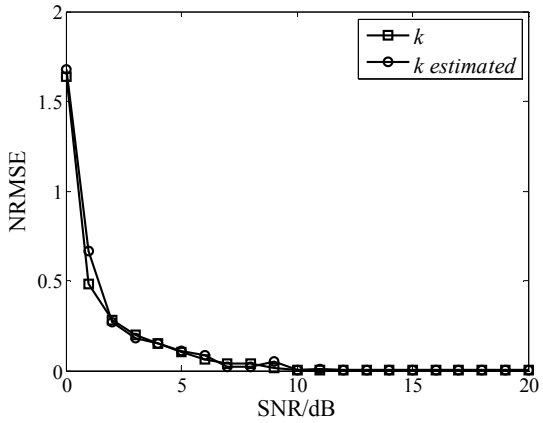

Fig. 5 NRMSE VS SNR of the code rate

In Fig.5, 'k' stands for $\Delta k = \hat{k} - k = 0$, 'k estimated' $\Delta k = \hat{k} - k \neq 0$.

It can be found by Table 1 and Fig 5 that when the SNR > 6dB, the NRMSE of the estimated code rate is less than 10^{-2}. The effect of $\Delta k = \hat{k} - k$ on the code rate estimation turns out to be not significant.

4.3 The effect of the parameter

From the equation (21), $\frac{1}{\xi(T_c)} = \frac{1}{0.5T_c^2}$, we find that $h_{\max}$ and T_c have an influence on the estimate of k. On the one hand, obviously, with the increase of T_c, the precision of $\hat{k}$ will improve. That is to say, for the longer pulse, we can get the more accurate estimation. On the other hand, we have pointed out that the estimate of $h_{\max}$ depends on the selection of window. Since the peak location for accurate frequency estimate is needed, we choose the rectangular window whose main lobe is narrow and easy for identification. The simulation results of different T_c and windows are shown in Fig 6.

Meanwhile, the estimate of the code rate is related to τ . To reduce the computation cost, we should assign a suitable time delay τ_{best} and descend the searching procedure to one dimension. The simulation results show that τ_{best} is approximately half of the code width T_1 finally. Moreover, we consider the error transfer. In our processing, the estimate of k can have an effect on the estimate of the code rate. When $\Delta k = \hat{k} - k \neq 0$, there will be a term $e^{j(\pi \Delta k t^2)}$. This term is a baseband LFM signal which has also been proven to be cyclostationary, the modulus of cyclic autocorrelation function $R^{\alpha}_{LFM}(\tau)$ is

$$\left|R^{\alpha}_{LFM}(\tau)\right| = \begin{cases} 2\pi\delta(2\pi\alpha + 2\pi\Delta k\tau), & \alpha \neq 0 \\ 0, & otherwise \end{cases} \tag{23}$$

where $|\tau| \neq 0$ .It is a Dirac function that is nonzero when $\alpha = -\Delta k\tau$ .Because Δk is very small, the effect of the impulse on the estimate of the code rate can be ignored.

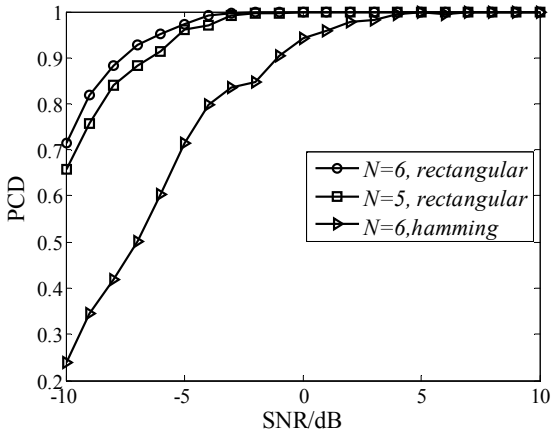

Fig. 6 PCD VS SNR of the chirp rate of different parameters

In Fig.6, 'N=6, rectangular' stands for N=6, the rectangular window, 'N=5, rectangular' N=5, the rectangular window, 'N=6, hamming' N=6, the hamming window. According to the simulation results, we verify the conclusion that the longer pulse and the rectangular window have the better performance of k estimation.

5 Conclusion

We investigate the S-cubed signal and build its signal model. In order to intercept the S-cubed, an parameter estimation algorithm is proposed based on MMST spectrum. The algorithm is feasible for both single and multi-components S-cubed signal. The next work will widen MMST to be used in signal detection or automatic modulation configuration (AMC) for the other kinds of hybrid modulation signals.

References:

[1] D. Celik, I. Altunbas, U. Aygolu, Performance improvement in coded cooperation systems using FSK/PSK modulation, *IEEE Signal Processing and Communications Applications Conference*, 2009, pp. 864-867.

[2] D. Celik, I. Altunbas, U. Aygolu, FSK/PSK Modulated Coded Cooperation Systems, *International Conference on Communication Theory, Reliability, and Quality of Service*, 2010, pp. 9-14.

[3] H.B.Yang, J.J. Zhou, F.Wang, Design and analysis of Costas/PSK RF stealth signal waveform, *IEEE CIE International Conference on radar*, 2011, pp. 1247-1250.

[4] Y.S. He, Y.F.Cheng, G.Wu, et al, Performance analysis of FFH/BPSK system with partial band noise jamming and channel estimation error in high-mobility wireless communication scenarios, *Chinese Science Bulletin*, Vol.59, No.35, 2014, pp. 5011-5018.

[5] D. Lynch, *Introduction to RF stealth*, USA: SciTech Publishing, 2004.

[6] S. Chetwani, A. Papandreou-Suppappola,Time-varying interference suppression in communication systems using time-frequency signal transforms, *Conference Record of the Thirty-Fourth Asilomar Conference on Signals, Systems and Computers*, 2000,1, pp. 460-464.

[7] H.Shen, A. Papandreou-Suppappola, Wideband time-varying interference suppression using matched signal transforms, *IEEE Transactions on Signal Processing*, Vol.53, No.7, 2005, pp. 2607-2612.

[8] Y.P. Li, Y.Xiong, B.Tang, SMSP jamming identification based on Matched Signal transform, *International Conference on Computational Problem-Solving*, 2011, pp. 182-185.

[9] X.D.Zeng, B.Tang, Y.Xiong, Interception algorithm of S-cubed signal model in stealth radar equipment, *CJA*, Vol. 25, No. 3, 2012, pp. 416-422.

[10] X.D.Zeng, Y.Xiong, W.Zhang, et al, Feature parameter extraction approach with the stealth S-cubed radar signal, *IEEE CIE International Conference on radar*, 2011, pp. 1813-1816.

[11] J.Yan, H.B.Ji, Cyclic autocorrelation based blind parameter estimation of PSK signals, *International Conference on ITS*

Telecommunications Proceedings, 2006, pp.1293-1296.